Thermal and mechanical analysis of low-temperature and low-pressure silver-based sintered thermal joints

Krzysztof Jakub Stojek and Jan Felba
Faculty of Microsystems Electronics and Photonics, Wroclaw University of Science and Technology, Wroclaw, Poland
Damian Nowak
Wrocław University of Technology, Wroclaw, Poland, and
Karol Malecha, Szymon Kaczmarek and Patryk Tomasz Tomasz Andrzejak
Wrocław University of Science and Technology, Wrocław, Poland

Abstract

Purpose – This paper aims to perform thermal and mechanical characterization for silver-based sintered thermal joints. Layer quality affects thermal and mechanical performance, and it is important to achieve information about how materials and process parameters influence them.

Design/methodology/approach – Thermal investigation of the thermal joints analysis method was focused on determination of thermal resistance, where temperature measurements were performed using infrared camera. They were performed in two modes: steady-state analysis and dynamic analysis. Mechanical analysis based on measurements of mechanical shear force. Additional characterizations based on X-ray image analysis (image thresholding), optical microscope of polished cross-section and scanning electron microscope image analysis were proposed.

Findings – Sample surface modification affects thermal resistance. Silver metallization exhibits the lowest thermal resistance and the highest mechanical strength compared to the pure Si surface. The type of dynamic analysis affects the results of the thermal resistance.

Originality/value – Investigation of the layer quality influence on mechanical and thermal performance provided information about different joint types.

Keywords Thermography, Thermal joints, Silver nanoparticles, Mechanical and thermal characterization, Electronic packaging

Paper type Research paper

Introduction

Higher clock frequencies in relation to the miniaturization of active electronic devices causes the generation of a large amount of heat. Effective heat transfer through thermal joints has become one of the most crucial topics in microelectronics packaging, where the characterization of modern materials is very important for development of improved materials and techniques. Typical materials such as solders and thermally conductive adhesives are no longer sufficient, due to their limitation of use to solderable surfaces (in the case of solders), or limited thermal conductivity of adhesives when they are joined to other surfaces (Xiao, 2013; Göbl and Faltenbacher, 2010). The use of high-conductivity materials with acceptable mechanical properties for thermal joint manufacturing is more popular nowadays, where its role is to decrease the active element temperature by effective heat removal in the conductive heat transfer mode. The role of such materials is to fill micro-sized gaps with highly conductive materials, improve contact area and, as a result, improve heat transfer, which corresponds to lowering the thermal resistance. Silver is a very interesting material for heat removal applications because it has a high relative thermal conductivity (highest among metals), and silver oxides are thermally and electrically conductive. Sintering is also interesting for heat removal applications because, with the use of silver, it is possible to manufacture a highly conductive layer with high reliability, and most importantly, the layer has higher electrical and thermal parameters than solders, especially considering the pressure-assisted technique.

Sintering technology has a solid theoretical basis and has been investigated and tested for several years (Zhang and Lu, 2002; Bai, 2005; Xiao, 2013; Fu *et al.*, 2014). As a result, this technology is successfully applied in electronic packaging (Lu *et al.*, 2007; Göbl and Faltenbacher, 2010; Wang *et al.*, 2013; Fu *et al.*, 2014; Welker *et al.*, 2015; Liu *et al.*, 2018; Siow, 2019; Hng *et al.*, 2020) where shear strength and both thermal and electrical resistivity are important parameters of joints. In most

The current issue and full text archive of this journal is available on Emerald Insight at: **https://www.emerald.com/insight/0954-0911.htm**

Soldering & Surface Mount Technology
35/1 (2023) 9–17
Emerald Publishing Limited [ISSN 0954-0911]
[DOI 10.1108/SSMT-06-2021-0042]

Received 30 June 2021
Revised 30 October 2021
23 February 2022
Accepted 16 March 2022

research works, the mechanical strength of the joint is the main criterion of the technology. Analysing many articles, it was shown (Felba, 2018) that the highest shear strength values were obtained when both joined surfaces were metallized with silver (average value of 42 MPa) and gold (30 MPa), or there were different metallizations of the surfaces to be joined; Ag + Au (26 MPa), Ag + Cu (52 MPa), Au + Cu (64 MPa). Joints with Ag + Ag metallization were the most often tested as those with sintered Ag on copper metallization, as well as using sintered copper nanoparticles required special joining procedures because copper is easily oxidized (Siow *et al.*, 2019; Zhang *et al.*, 2021; Chen and Siow, 2021). Many authors assumed that sintered Ag can be treated as a very good electrical and thermal conductor, and the exact methods of measuring the thermal conductivity of the joint itself (i.e. a synthesized layer and both metallizations) are not widely presented. However, it would be interesting to find a correlation between the mechanical and thermal parameters of the joints and to evaluate the effect of the metallized layers on the heat flow. The aim of work reported in this paper was to find these relationships. The quality of thermal joints depends on the materials used and technological parameters where, among a number of factors (Felba, 2018), it seems that most important ones are process temperature and time, the pressure assistance and material composition. Such conclusions were also the result of previous works (Stojek *et al.*, 2017a, 2017b). The process used for the research shown herein was done at temperatures below 300°C with pressure assistance at a level lower than 1 MPa. Compared to typical sintering, this process may be considered as low temperature and low pressure.

The lowest possible thermal resistivity along with simultaneous acceptable mechanical strength are the two main requirements for thermal joints in electronic packaging. The materials and technological parameters affect the quality of the sintered layer, which directly corresponds to the mechanical and thermal performance. Previous observations showed that it was important to use a statistically representative population of samples. Thermal and mechanical performance relies on layer quality; therefore, after sample preparation, X-ray inspection (as a non-destructive method) was performed and image acquisition was used for further analysis. For thermal characterization, an infrared camera was used. This allowed contactless, relatively low cost, fast and repeatable measurements. Two types of thermal characterizations were performed:

1 steady-state analysis, where samples were supplied with electrical power and thermal measurements were performed when temperature values became stable; and
2 dynamic analysis, where samples were stimulated with variable signals and their response was measured.

Mechanical analysis included scanning electron microscopy and optical microscopy of polished cross-sectional images, but shear force measurements were performed in a typical tensile machine. X-ray image analysis was done using the image thresholding method to evaluate real contact areas in context to determine relative coverage.

Samples and sintering parameters

The analysed samples comprised a heat source, a heat receiver and a silver layer between them. Both the heat source and the heat receiver were self-manufactured bare-die silicon chips with dimensions of 5 × 5 mm and thickness of 3 mm. The basis of the sintered layer can be nanoparticles (Kähler *et al.*, 2011; Guo *et al.*, 2015), microsized particles (Zheng *et al.*, 2012; Takemasa *et al.*, 2016) or a mixture of the two (Kuramoto *et al.*, 2010; Matkowski *et al.*, 2015). After previous experiences, a mixture was chosen. The silver paste composition for sintering was 95 Wt.% silver particles (60 to 40 nano- to micro-flake ratio) and 5 Wt.% epoxy resin. The average size of the silver nanoparticles was 70 nm and the micro-sized flakes averaged 15 μm. It seems obvious that the use of epoxy resin interferes with the standard sintering process, mainly by introducing components that can adversely affect the structure of the joint, resulting in a reduction in its mechanical strength. But the epoxy resin's role in the paste composition was to enable joint manufacturing to different surfaces, even non-metallized. This made it possible to compare the joint properties of different surfaces. The paste was applied to the heat receiver by stencil printing and then the heat receiver was placed on the heat source. The same paste was used for all tests (with the same viscosity), so the same amount of paste was dispensed, which should result in the same thickness of the sintered layer of all samples. Unfortunately, after the sintering process, the joined surfaces were not evenly covered with the Ag layer (Figure 10), which may have caused differences in heat transfer for samples made under the same conditions. Therefore, statistical studies were necessary; between 12 and 20 samples were processed for each sample type. In such a manner, four types of structure were manufactured:

1 non-metallized (silicon chip – sintered Ag – silicon chip);
2 silver-plated (silicon chip + Ag metallization – sintered Ag – silicon chip + Ag metallization);
3 copper-plated (silicon chip + Cu metallization – sintered Ag – silicon chip + Cu metallization); and
4 oxidized (silicon chip + SiO_2 – sintered Ag – silicon chip + SiO_2).

The sintering process was carried out at 230°C for 60 min with 54 min of heating at a 4°C/min rate in air. The process was pressure assisted at 0.5 MPa. Sintered samples were attached to the printed circuit board (PCB) using electrically conductive adhesive, and its role was to supply electrical power to the samples. Figure 1 shows the structure of the samples.

Additional layer manufacturing and characterization

The purpose of the different layers on the silicon substrate manufacturing was to affect heat transfer. In such multilayer structures, each material had its own thermal resistance and thermal contact resistance between two neighbouring layers (Felba, 2011) additionally limited the heat flow. From a theoretical point of view, the lower the number of material layers, the lower the thermal resistance. The removal of semiconductor metallization was also beneficial, because the

Figure 1 Sample structure – schematic view

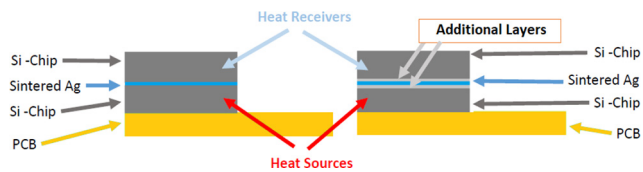

manufacturing of thermal joints would be cheaper (each process generates cost). So, it was important to determine how semiconductor metallization removal affects mechanical and thermal performance. As previously mentioned, the typical semiconductor surface metallization for silver sintering is a silver layer. Sintering of the silver paste to the silver semiconductor surface might create a strong bond because there is no coefficient of thermal expansion impact to cause joint stress.

The aim was to investigate the impact of different semiconductor surface materials on heat transfer through thermal joints and should be the effect of material type, not its thickness. As for silicon semiconductor chips, the easiest modification was to oxidize the surface. The process was carried out for 1 h in 1000°C. To determine the silicon dioxide thickness, a focused ion beam (FIB) was used for material removal and then scanning electron microscope measurements were performed. In the case presented in Figure 2, the mean thickness of the silicon dioxide was 2.07 μm.

The silver and copper layers were deposited by magnetron sputtering. After the process, the layers were cured at 800°C to perform metal diffusion to silicon. Such a standard procedure aims to improve the mechanical strength and reduce the electrical resistance between them. To perform thickness measurements, polished cross-sections were made. Both the sintered silver layer and also the metallization thickness were measured. The mean thickness of the silver and copper were 1.26 and 1.46 μm, respectively (Figure 3).

Thermal analysis

The supplied electrical power was converted to heat inside the heat source. Heat was transferred to the heat receiver through the sintered layer via conduction. Emitted infrared radiation (IR) was used for thermal measurements of the source (T_S) and receiver (T_R) surfaces using an infrared thermographic camera, Flir A40m. Using an IR camera has a number of advantages; measurements are contactless, so heat flow is not affected. The method is also relatively fast and cheap. Source and receiver temperatures were measured for given areas and their mean values were taken into account for analysis.

As convection is strongly connected with gravity, sample orientation affects thermal measurements. In Figure 1, the heat source was placed at the bottom of the sample (in relation to the heat receiver), and the heat lost in the heat source may increase the temperature of the sample by convection. To remove heat loss in the form of convection measurements, the procedure may be performed in a vacuum chamber. However, performing infrared measurements is difficult, because they require use of an IR window, which is transparent to the radiation spectra, and there are always losses of transmitted optical signal (Stojek *et al.*, 2020, 2019). In the presented research, the orientation of the sample ensured minimal heat receiver heating via convection and keeping the same distance between the camera lens and both analysed surfaces, the camera was placed above the sample (as shown in Figure 4). The infrared camera was calibrated before measurements as factors like atmospheric humidity and temperature, distance, reflected temperature and the external optics could have an impact and may affect the IR thermal analysis. The samples' surfaces were covered with an anti-glare layer with known emissivity (0.98).

Thermal steady-state analysis

The steady-state analysis method was performed when the thermal parameters became stable and the temperature changes of the source (T_S) and receiver (T_R) were not significant. Temperature differences (ΔT) between source and receiver were calculated. At the same time, the given power (P)

Figure 2 Silicon dioxide SEM images and measurements

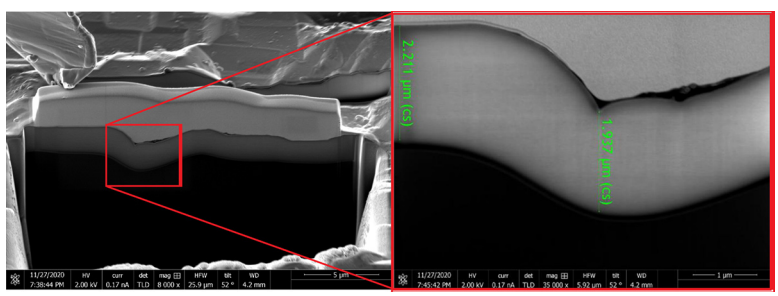

Figure 3 Silver and copper metallization microscope measurements

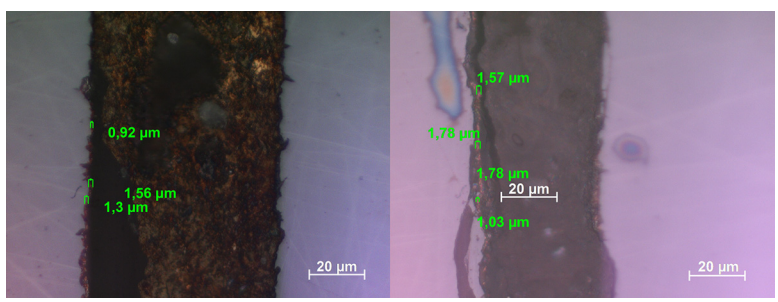

Figure 4 Steady-state thermal analysis method scheme

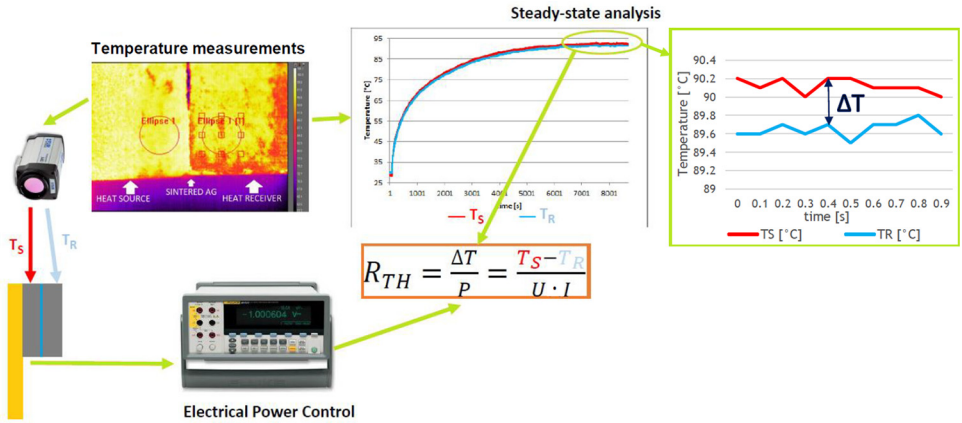

measurements were made in the form of current (I) and voltage (U) measurements (Figure 4). The thermal response was a result of thermodynamic processes that became stable in time, which meant that current flow through the sample, voltage and power were steady and temperatures on the source and substrate were also steady. According to the thermal and electrical information, it was possible to calculate the thermal resistance using the following formula:

$$R_{TH} = \frac{\Delta T}{P} = \frac{T_S - T_R}{U \cdot I} \quad (1)$$

Voltage, current, source and substrate temperatures were measured. Then the power and temperature differences were calculated and finally, the thermal resistance was calculated for each sample. Then, for each structure type (non-metallized, silver-plated, copper-plated and oxidized), the average thermal resistance was calculated, as well as the standard deviation. Examples of mean thermal resistance calculations for non-metallized structures are presented in Table 1. Three other sets were calculated in the same manner.

Thermal IR contactless analysis was performed with ± 2°C or ± 2% accuracy (higher among both for given conditions). The thermal sensitivity was 0.08°C at 30°C. In this case, values were measured with a precision of 2%, but the lowest distinguishable value was 0.1°C, which was satisfactory for the comparative analysis in this work. The steady state was determined if the source temperature reached approximately 100°C and was stable for at least 1 min. The mean temperature difference is presented in the Figure 5.

Statistical analysis demonstrated that the non-metallized structures showed the lowest temperature difference between source and receiver. The highest was reached for copper-plated structures, even higher than for oxidized structures, because silicon dioxide's thermal conductivity is approximately two orders lower than copper. However, in the sample preparation procedure, it was mentioned that the sintering process was performed in air and also copper was heated to 800°C to diffuse it to the silicon surface, where, in fact copper oxide probably appeared. Moreover, typical copper oxide (CuO) has a thermal conductivity one order of magnitude higher than silicon dioxide (SiO_2), so this

Table 1 Example for non-metallized structure thermal resistance analysis – based on voltage, current source and receiver temperature measurements and power, temperature difference calculations

	Voltage	Current	Power	Source temperature	Receiver temperature	Temperature difference	Thermal resistance
	U	I	P	T_S	T_R	ΔT	R_{TH}
Sample no	[V]	[A]	[W]	[°C]	[°C]	[°C] or [K]	[K/W]
1	1.21	1.42	1.72	99.7	98.9	0.8	0.46
2	1.26	1.64	2.07	99.8	99.1	0.7	0.34
3	1.22	1.34	1.63	100.2	99.3	0.9	0.55
4	1.52	0.64	0.98	99.6	98.4	1.2	1.23
5	2.96	0.36	1.08	100	98.2	1.8	1.67
6	7.31	0.16	1.15	100.1	99.4	0.7	0.61
7	4.41	0.18	0.78	99.2	98.1	1.1	1.41
8	1.52	4.12	6.24	100.3	99.1	1.2	0.19
9	1.48	2.28	3.37	100.5	98.5	2	0.59
10	1.64	2.91	4.76	100	98.8	1.2	0.25
11	1.35	1.82	2.46	100.1	98.7	1.4	0.57
						mean R_{TH}	0.72
						std. dev.	0.47

Figure 5 Steady-state analysis average temperature difference

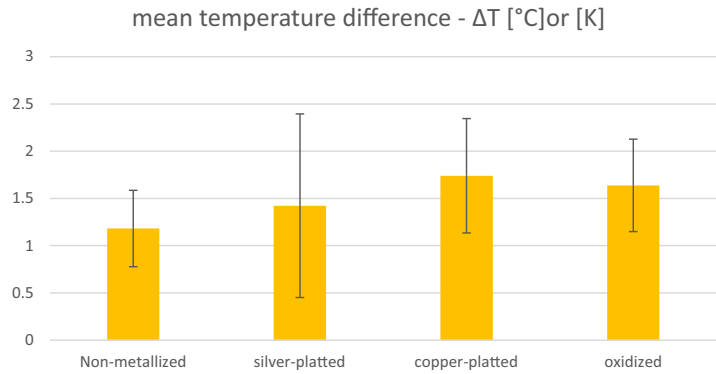

needs further research. Extending thermal measurements with supplied power measurements, the thermal resistance calculation was performed (according to formula 1) and presented in Figure 6.

The lowest thermal resistance was obtained for silver-plated samples and the highest for non-metallized structures. This may indicate that, with respect to thermal requirements, it is worth manufacturing silver metallization on semiconductor substrates.

Thermal dynamic analysis

The higher thermal resistance difference was between non-metallized and silver-plated structures (Figure 6). In such a manner, these samples were analysed using a thermo dynamic analysis method. In such a case, samples were stimulated with different types of signals, e.g. sine, square and pulse. The infrared camera detector operated at 50 Hz maximal, so the detected signals should not exceed 25 Hz to avoid aliasing. With such restrictions, measurements were performed in quasilogarithmic scale frequencies: 0.1; 0.2; 0.3; 0.4; 0.5; 0.6; 0.7; 0.8; 0.9; 1; 2; 3; 4; 5; 6; 7; 8; 9; 10; 15; 20 and 25 Hz. As mentioned before, three types of signals were used:

1 Sine – the stimulating signal was in fact half of a sine wave, using diode for signal rectification. As a result, there was stimulation in a given time and thermal response,
2 Square – a controlling MOSFET transistor supplied given electrical power to the structures using a square wave signal that had a 50% duty cycle. It was basically turning the power supply on and off periodically,
3 Pulse – a controlling MOSFET transistor that supplied given electrical power to the structures using a square wave signal, but this time it had a 20% duty cycle, and again, it was turning the power supply on and off periodically.

Figure 6 Steady-state average thermal resistance

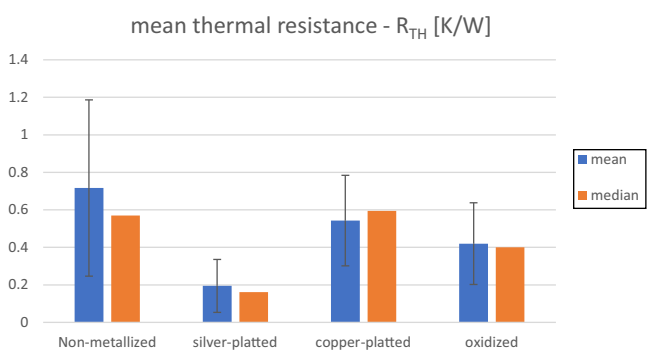

The supplied periodic energy improved the system temperature and after a given number of cycles the thermodynamic response became steady, even with stimulating signal periodic operation. So, the heating curves varied by particular cycle, but there was no significant difference between next cycles and such a moment was taken for the analysis. For a given cycle, there were maximal temperatures on source and receiver, which were taken for thermal resistance calculations. The supplied power was measured using a Fluke 8846a digital multimeter, and the thermal resistance was calculated according to the formula for each frequency (Figure 7). Then the average thermal resistance for each sample was calculated.

All dynamic results were compared with steady-state analysis. The lowest thermal resistance was reached for the square wave and the highest for sine wave stimulation. Square wave stimulation thermal resistance results were lower, and sine wave was higher than the steady-state thermal resistance. Pulse stimulation was comparable to steady-state analysis. It is clearly visible that using different methods may affect the results of the thermal resistance calculations. However, from these studies, it can be concluded that, generally, the thermal resistance of metallized surfaces was lower than that of non-metallized surfaces. Especially large differences occurred when comparing pure silicon surfaces with those covered with silver metallization. This means that the contact thermal resistance between the Si surface and the sintered Ag layer played a greater role than the sum of the thermal resistances Si - Ag (contact between Si and metallization), Ag (metallization) and Ag - Ag (between metallization and sintered layer). In the case of non-metallized, Cu-plated and oxidized surfaces, the differences in the thermal resistances of the joints were insignificant, and it was difficult to conclude which type of thermal resistance was dominant.

Mechanical analysis

In addition to thermal characterization, it is important to determine how different structures affect the mechanical parameters of joints and the standard shear test describes the

Figure 7 Thermal dynamic analysis method scheme

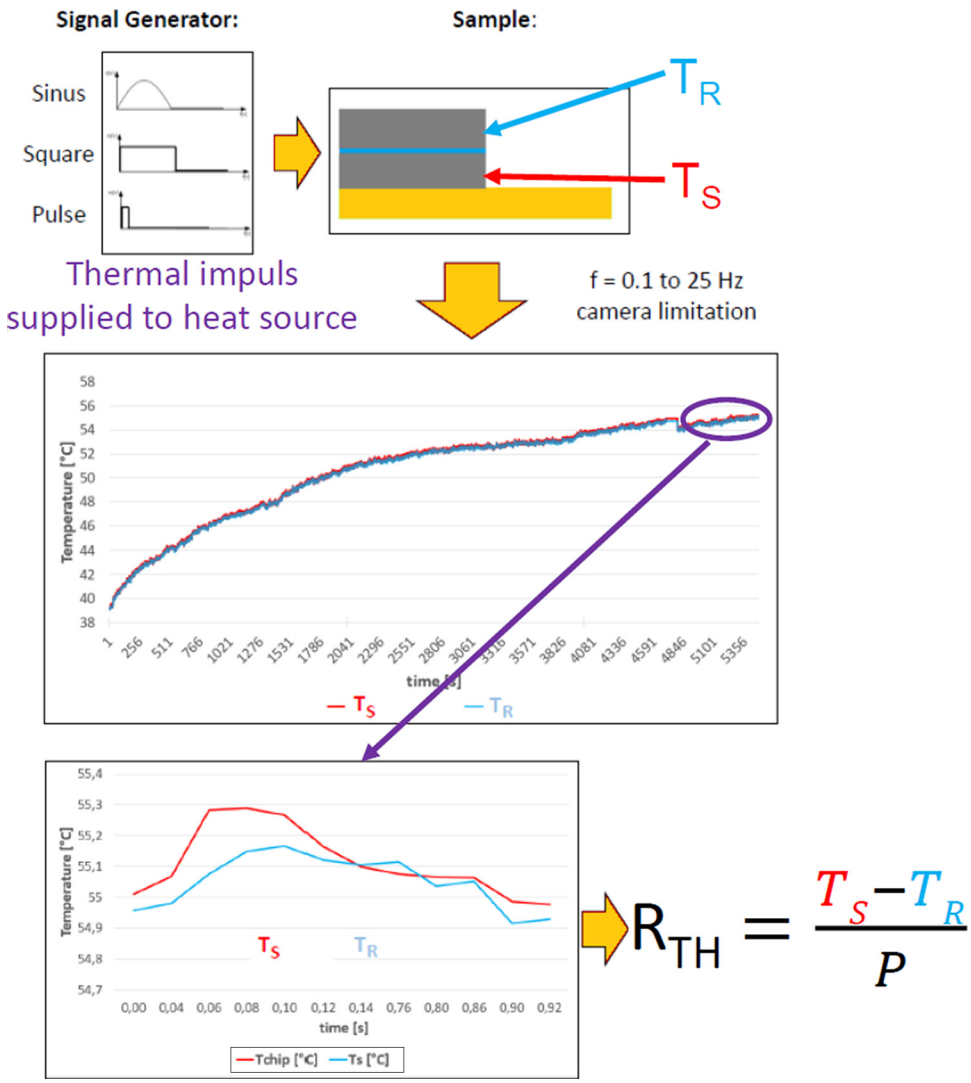

layer strength on shear stress. Therefore, shear force measurements were performed in a typical tensometer, and the results are presented in Figure 9.

In general, the mechanical strengths of the tested joints were significantly lower than in the case of standard sintered connections of metallized surfaces. This was probably due to the presence of an epoxy resin. However, relative differences could be observed; the highest mechanical strength was obtained for silver-plated structures and a little lower for non-metallized structures.

Taking into account both important parameters of joints, i.e. thermal resistance and mechanical strength, joints with Ag metallization were the best. However, in cases where heat transfer may be slightly limited, non-metallized joints can be applied. The advantage of these joints is the limitation of technological steps (metallization) and, therefore, lower cost. When the chosen non-metallized, Cu-plated or oxidized joints are considered, the first of the mentioned joints seems to have many more advantages.

Quality of sintered Ag layer

Ideally, the sintered Ag layer should be homogeneous, of a constant thickness and completely cover both surfaces to be joined. Unfortunately, in practice, the layer after the thermal process was heterogeneous and contained many voids. It was the result of the processes that took place during sintering, where the Ag paste was trapped between the surfaces to be joined, in particular the evaporation of volatile components of the paste and the change in volume (Xiao, 2013). Therefore, it is extremely important to know the structure of sintered layers and their differences, when joining different types of surfaces. In the case of large differences, the previous considerations regarding the influence of thermal resistances (contact and individual layers) may be wrong. Simply, defects and imperfections of the layer can be of dominant importance in heat transfer.

For a quantitative sintered layer quality approach, X-ray image thresholding software was used. As a non-destructive method, X-ray images were obtained after sample preparation. At first, the software had an option to calibrate the sample

Figure 8 Dynamic analysis thermal resistance

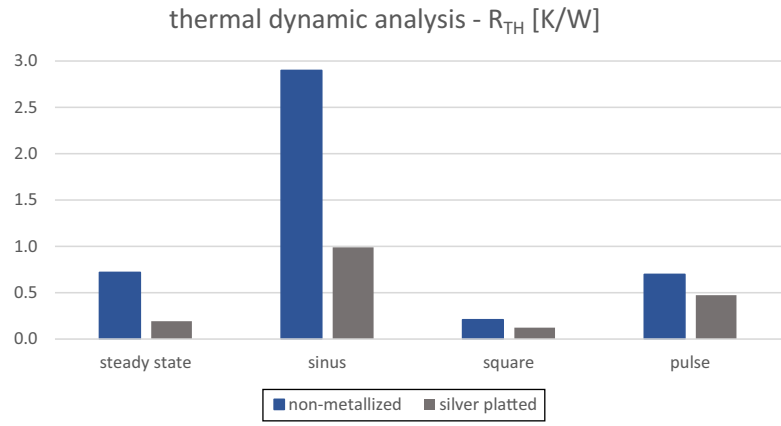

Figure 9 Average shear force measurements results

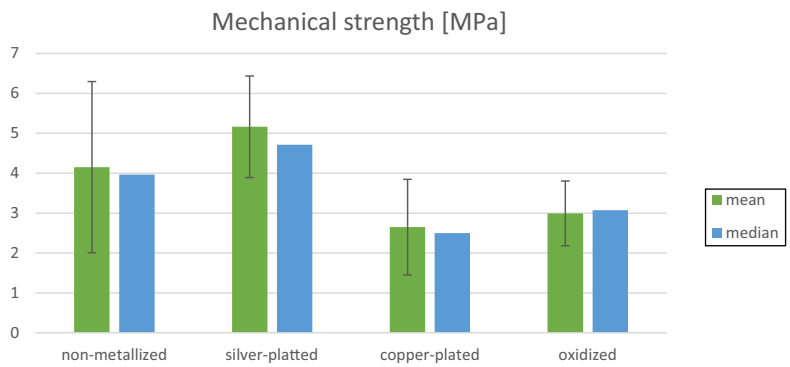

dimensions and to allow one to determine the real sizes of defects. Each X-ray image in grey scale was thresholded with a given, well-known area, where it was certain that there was silver; areas near sample edges were omitted. The darker areas in Figure 10 are silver, and brighter areas are the lack of silver, mostly epoxy resin or void spaces. The software had two options for representation of thresholded images: contour mode – basic mode, where the software marked areas detected as silver by using contour colour change (figure middle) and colour swap mode, where the software changed the colour of all pixels classified as silver (figure right). The threshold values were selected and used according to the measurements made by the user in the software and their selection was arbitrary.

Thanks to dimension calibration and silver detection via image thresholding, it was possible to determine the silver area's relationship to the whole contact area and as a result, the percent of coverage by silver, i.e. relative coverage. Analysis was performed for all samples, where the mean value and standard deviation were calculated. The results are shown in Figure 11.

Relative coverage exceeded 50% for all types of structures. It was a surprising result showing that only half of the joint surfaces were real joints (there is thus a challenge to improve

Figure 10 X-ray image thresholding: left – exemplar X-ray image in grey scale, middle – image thresholded in contour mode, right – image thresholded in colour swap mode

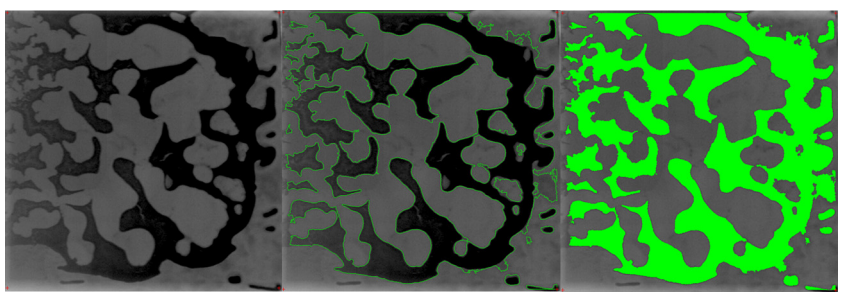

Figure 11 X-ray image coverage calculations – thresholding results

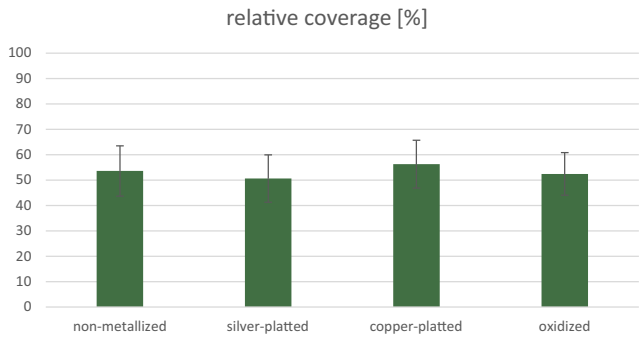

this result). Nevertheless, more positively, the relative coverage differed by less than 10%, for all tested surfaces. This meant that the previous considerations on the influence of individual thermal resistances were not burdened with an error resulting from the quality of the sintered layer.

An additional conclusion from the research is the difficulty in assessing the impact of the thickness of the synthesized layer on the quality of the joints. Typically, thickness is measured optically on polished cross-sections when the cut line is random. It can be seen from Figure 10 that the cut line can pass through either the Ag layer or through an empty space. In such manner, the sintered layer thickness was measured, and the results showed significant differences in the assessment of the thickness of the layers: 25 μm for non-metallized surfaces, 69 μm (silver-plated), 42 μm (copper-plated) and 21 μm (oxidized).

Conclusions

The aim of this work was to perform thermal and mechanical characterization of silver-based sintered thermal joints. Two silicon structures were joined, but the direct-joint surfaces were different. Four types of samples were manufactured: non-metallized surfaces (pure silicon chips), silver-plated surfaces, copper-plated surfaces and silicon oxidized surfaces. The silicon chips were joined using a paste that had 95 Wt.% of silver particles in (60 to 40 nano- to micro-flakes ratio) and 5 Wt.% epoxy resin. The size of the silver nanoparticles averaged 70 nm and the micro sized flakes averaged 15 μm. The sintering process was carried out at 230°C for 60 min with 54 min of heating at a rate of 4°C/min. The process was pressure assisted at 0.5 MPa.

The tested chips served as heat sources and heat receivers. Emitted infrared radiation was used for thermal measurements of source and receiver surfaces using infrared thermographic camera. According to achieved thermal and electrical (heat source power) information, it was possible to calculate the global thermal resistance of the joints. Theoretically, such thermal resistance is the sum of the metallic layer resistances and the contact resistances. The aim of the research was to assess whether fewer layers of materials contributed to lower thermal resistance. Additionally, the shear forces of the joints were measured in a typical tensile machine.

It was found that the thermal resistance of the metallized surfaces was lower than that of the non-metallized surfaces. Especially large differences occurred when comparing pure Si surfaces with those covered with Ag metallization. This meant that the contact thermal resistance between the Si surface and the sintered Ag layer played a greater role than the sum of the thermal resistances of Si - Ag (contact between Si and metallization), Ag (metallization) and Ag - Ag (between metallization and sintered layer). In the case of non-metallized, Cu-plated and oxidized surfaces, the differences in the thermal resistance of the joints were insignificant, and it was difficult to conclude which type of thermal resistance was dominant. Taking into account both important parameters of the joints, thermal resistance and mechanical strength, joints with Ag metallization were the best. However, in cases where heat transfer may be slightly limited, non-metallized joints can be applied. The advantage of these joints is the limited number of technological steps (metallization) and therefore, lower cost. When the chosen non-metallized, Cu-plated or oxidized joints were chosen, the first of the mentioned joints seemed to have many more advantages.

References

Bai, G. (2005), "Low-temperature sintering of nanoscale silver paste for semiconductor device interconnection", PhD dissertation, Virginia Tech, Blacksburg, VA.

Chen, T.F. and Siow, K.S. (2021), "Comparing the mechanical and thermal-electrical properties of sintered copper (Cu) and sintered silver (Ag) joints", *Journal of Alloys and Compounds*, Vol. 866, p. 158783.

Felba, J. (2011), "Thermally conductive adhesives in electronics", in Alam, M.O. and Bailey, C. (Eds), *Advanced Adhesives in Electronics: Materials, Properties and Applications*, Woodhead Publishing, pp. 15-52.

Felba, J. (2018), "Technological aspects of silver particle sintering for electronic packaging", *Circuit World*, Vol. 44 No. 1, pp. 2-15.

Fu, S., Mei, Y., Lu, G.-Q., Li, X., Chen, G. and Chen, X. (2014), "Pressureless sintering of nano silver paste at low temperature to join large area (_100 mm2) power chips for electronic packaging", *Materials Letters*, Vol. 128, pp. 42-45.

Göbl, C. and Faltenbacher, J. (2010), "Low temperature sinter technology; die attachment for power electronic application", *6th International Conference on Integrated Power Electronics System (CIPS)*, *Nuremberg*.

Guo, W., Zeng, Z., Zhang, X., Peng, P. and Tang, S. (2015), "Low-temperature sintering bonding using silver nanoparticle paste for electronics packaging", *Journal of Nanomaterials*, Vol. 2015.

Hng, W.S., Kim, M.S. and Oh, C. (2020), "Low-pressure silver sintering of automobile power modules with a silicon-carbide device and an active-metal-brazed substrate", *Journal of Electronic Materials*, Vol. 49 No. 1, pp. 188-195.

Kähler, J., Heuck, N., Palm, G., Stranz, A., Waag, A. and Peiner, E. (2011), "Low-pressure sintering of silver micro and nanoparticles for a high temperature stable pick & place die attach", *18th European Microelectronics and Packaging Conference*, *Brighton*.

Kuramoto, M., Ogawa, S., Niwa, M., Kim, K.-S. and Suganuma, K. (2010), "Die bonding for a nitride light emitting diode by low-temperature sintering of micrometer

size silver particles", *IEEE Transactions on Components and Packaging Technologies*, Vol. 33 No. 4, pp. 801-808.

Liu, W., An, R., Wang, C., Zheng, Z., Tian, Y., Xu, R. and Wang, Z. (2018), "Recent progress in rapid sintering of nano silver for electronics applications", *Micromachines 2018*, Vol. 9 No. 7, p. 346, doi: 10.3390/mi9070346.

Lu, G.Q., Calata, J.N., Lei, G.Y. and Chen, X. (2007), "Low temperature and pressureless sintering technology for high performance and high-temperature interconnection of semiconductor devices", *International Conference on Thermal, Mechanical and Multi-Physics Simulation Experiments in Microelectronics and Micro-Systems*, EuroSime.

Matkowski, P.K., Falat, T. and Moscicki, A. (2015), "Reliability of interconnections made of sintered silver Nano particles", *ASME International Technical Conference and Exhibition on Packaging and Integration of Electronic and Photonic Microsystems*, *San Francisco, CA*.

Siow, K.S. (2019), *Die-Attach Materials for High Temperature Applications in Microelectronics, Packaging Materials, Processes, Equipment and Reliability*, Springer.

Siow, K.S., Chua, S.T., Beake, B.D. and Zuruzi, A.S. (2019), "Influence of sintering environment on silver sintered on copper substrate", *Journal of Materials Science: Materials in Electronics*, Vol. 30 No. 6, pp. 6212-6223.

Stojek, K.J., Felba, J., Nicolics, J. and Wołczyński, D. (2020), "Impact of convection on thermo graphic analysis of silver based thermal joints", *Soldering & Surface Mount Technology*, Vol. 32 No. 4, pp. 241-246.

Stojek, K., Felba, J., Fałat, T. and Moscicki, A. (2017a), "Different aspects of non-metalized silicon dies joining with using low temperature and low pressure sintered silver nanoparticles", *40th International Spring Seminar on Electronics Technology*, *Sofia*.

Stojek, K., Felba, J., Fałat, T., Kiliszkiewicz, M. and Moscicki, A. (2017b), "The materials and technology parameters influenced on the mechanical properties of low temperature sintered silver joints", *21st European Microelectronics and Packaging Conference (EMPC) & Exhibition*, *Warsaw*.

Stojek, K., Felba, J., Fałat, T., Nowak, D., Mościcki, A. and Surmiak, A. (2019), "Heat transfer efficiency measurements with using thermography for low-temperature and low-pressure sintered silver joints", *7th Electronic System-Integration Technology Conference (ESTC)*, pp. 1-6.

Takemasa, T., Ueshima, M., Jiu, J. and Suganuma, K. (2016), "Die-bonding performance and mechanism based on the sintering of micro Ag paste for high power devices", *16th International Conference on Nanotechnology*, *Sendai*, pp. 377-380.

Wang, S., Li, M., Ji, H. and Wang, C. (2013), "Rapid pressureless low-temperature sintering of Ag nanoparticles for high-power density electronic packaging", *Scripta Materialia*, Vol. 69 Nos 11/12, pp. 789-792.

Welker, T., Müller, J., Krämer, F. and Wiese, S. (2015), "Electrical, thermal and mechanical characterization of low temperature, pressure-less sintered silver bond interfaces", *European Microelectronics Packaging Conference*, *Friedrichshafen*.

Xiao, K. (2013), "A diffusion-viscous analysis and experimental verification of the drying behavior in nanosilver-enabled low-temperature joining technique", Dissertation for Doctor of Philosophy, the Virginia Polytechnic, Institute and State University, Blacksburg, VA.

Zhang, B., Damian, A., Zijl, J., Van Zeijl, H., Zhang, Y., Fan, J. and Zhang, G. (2021), "In-air sintering of copper nanoparticle paste with pressure-assistance for die attachment in high power electronics", *Journal of Materials Science: Materials in Electronics*, Vol. 32 No. 4, pp. 4544-4555.

Zhang, Z. and Lu, G.Q. (2002), "Pressure-assisted low temperature sintering of silver paste as an alternative die attach solution to solder reflow", *IEEE Transactions on Electronics Packaging Manufacturing*, Vol. 25 No. 4, pp. 279-283.

Zheng, H., Calata, J., Ngo, K., Luo, S. and Lu, G.Q. (2012), "Low-pressure (< 5 MPa) low-temperature joining of large area chips on copper using nanosilver paste", *7th International Conference on Integrated Power Electronics Systems (CIPS)*, *Nuremberg*.

Corresponding author

Krzysztof Jakub Stojek can be contacted at: krzysztof.stojek@pwr.edu.pl